Trans Indian Inst Metals **(TP 1825)**
Vol.55, Nos. 1-2, February-April 2002, pp. 15-24

Investigations on the Microstructure and Quantification of Mechanical Properties of a Heat Treated Cu-bearing HSLA-80 Steel

P. K. Ray [1], **R. I. Ganguly** [2], **A. K. Panda** [2]

1 - Dept. of Applied Mechanics & Hydraulics,
Regional Engineering College, Rourkela 769008, INDIA.

2 - Dept. of Metallurgical Engineering,
Regional Engineering College, Rourkela 769008, INDIA.

Abstract :

An ULCB steel (named GPT) received from US Naval Research Laboratory has been characterised with respect to microstructure and mechanical properties. The effect of heat treatment parameters, such as austenitisation temperature, tempering temperature and tempering time has been studied. The microstructures obtained through different heat treatment have been studied through optical, scanning electron and transmission electron microscopes. The mechanical properties have been quantified with respect to heat treatment process parameters. Regression equations have been developed through 2^2 factorial design of experiments. These equations can be effectively used for optimisation purposes. Also it is possible, through these equations, to determine the heat treatment process variables for a desired combination of mechanical properties.

Keywords : HSLA-80 steel, heat treatment, mechanical properties

1. Introduction

HSLA 80 steel has come out as a replacement of Quenched & Tempered HY 80 grade steel. The improved technology has enabled the steel to become cleaner and more weldable [1]. The alloy chemistry of HSLA 80 suggests that it can admit alloying elements up to 4.5 wt %age [2]. The steel is designed with a view to having tensile properties such as minimum yield strength ~550 MPa with an elongation ≤ 18% and a V notch Charpy value of 85 Joule at -81°C [3]. The alloy composition for HSLA 80 steel is adjusted so as to combine the benefit of thermomechanical processing (resulting in grain refinement) along with judicious adjustment of strength through precipitation hardening with improved toughness at very low temperature [4]. The CCT curves for these steels indicate that there is a possibility of formation of combined microstructures consisting of Acicular ferrite / Bainite / low carbon martensite through controlled rolling and controlled cooling of the steel.

Owing to Cu content in the steel, this grade of steel responds to tempering after quenching [4-7]. In the first stage of tempering (450 °C), coherent precipitates of Cu clusters (presumably BCC) are observed. The matrix retains lath structure with dislocations. The clusters are not identifiable in TEM microstructures due to their fineness. The strength properties become the highest at this stage of tempering. However, the low-temperature impact value drops significantly at low temperature. During the second stage of tempering (500-600 °C), spherical ε-Cu (FCC) precipitates. The strength value decreases owing to partial recovery and coarsening of the precipitates with corresponding increase in impact values at low temperatures. Between 600-650 °C (stage III) the Cu precipitates change their shape from spherical to rod with appreciable recovery occurring in the microstructure [6]. During the fourth stage of tempering 650-700 °C, second generation austenite forms, which can be

revealed in the microstructure [6]. It is interesting to note that there is enhancement of strength and impact properties by tempering the steel in this region of time and temperature of tempering [5,7]. Therefore, optimization of properties is needed through control of process parameters such as temperature and time of tempering within this zone. Though some attempts have been made to optimize the properties through single factor experiments [5,6], less attempt has been made to quantity the effect of the variables on the strength and toughness properties. The present study attempts to quantify the effects of the processing parameters on mechanical properties such as YS, UTS, and Charpy impact values at low temperature to enable selection of the processing variables for the desired properties. Whenever necessary, structural characterization has been done by Optical, Scanning, and Transmission Electron Microscopy.

2. Experimental

The steel, designated GPT, was received from US Naval Research Laboratory (see Table 1 for composition) and is designated GPT. It was characterized with respect to inclusion content and grain size using Quantimet 570 image analysis system. AC_1 and AC_3 temperatures were measured using DTA, TMA and Dilatometer (Table 2). The heat treatment parameters studied were (i) austenitisation temperature, (ii) tempering temperature, (iii) tempering time.

Table - 1 Chemical composition of GPT steel

C	0.05
Mn	1.00
P	0.009
S	0.001
Si	0.34
Cu	1.23
Ni	1.77
Cr	0.61
Mo	0.51
Al	0.025
Cb	0.037
V	0.004
Ti	0.003

Table - 2. Ac_1 and Ac_3 values (Calculated and Experimental).

	Ac_1 (°C)		Ac_3 (°C)	
Steel	Calculated	Experimental	Calculated	Experimental
GPT	702	690	899	860

Temperatures were maintained within the accuracy limit of ±3°C. Microstructures of all the samples were examined by optical, scanning and Transmission Electron Microscopes. Fractured samples (Tensile & Charpy) were examined in Scanning Electron Microscope. Mechanical properties were determined in Instron testing unit (model 1195) for the as-received as well as heat treated samples adopting ASTM E-8-78 method.

In order to determine the region of optimum properties, heat treated samples were subjected to Charpy impact test at -50 °C. Charpy values were higher in the neighborhood of tempering temperature of 700 °C where the strength values were adequate i.e., YS ≥ 600 MPa or 85 ksi. It was therefore decided to design experimental matrices in this region and to form regression equations around tempering temperature of 650 °C.

3. Results & Discussions

The average grain size of the as-received steel was found to be between 7 to 8μm. The inclusion content of the steel was measured to be very low ($<10^{-4}$ Area fraction). This is attributed to very low content of P and S in the steel. The mechanical properties of the steel were found to be as follows:
YS = 636.7 MPa , UTS = 708 MPa ,
% Elongation = 30% on 25mm GL

Fig 1 shows Scanning Electron Microphotograph of as-received GPT steel. The microstructure indicates Bainitic / non-polygonal or acicular ferritic structure. The fractrograph of as-received tensile sample shows typical dimpled structure (Fig 2).

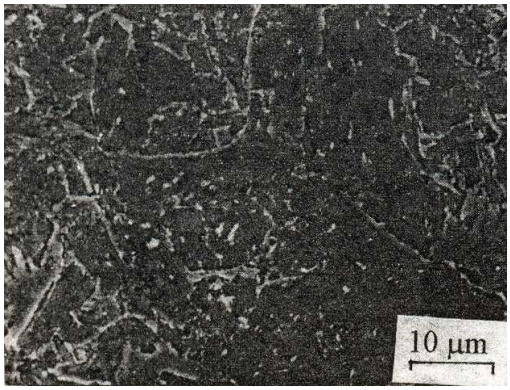

Fig. 1 - SEM of As-received steel

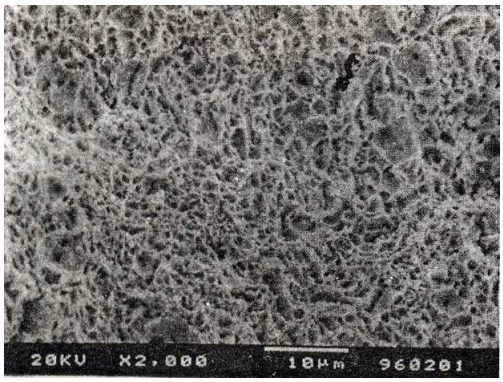

Fig. 2 - Fractograph of broken tensile specimen of As-received steel

Fig 3 shows the effect of tempering temperatures on hardness values of steel austenitised at 900, 950, 1000 °C for 1 hour followed by quenching in water and cooling in air.

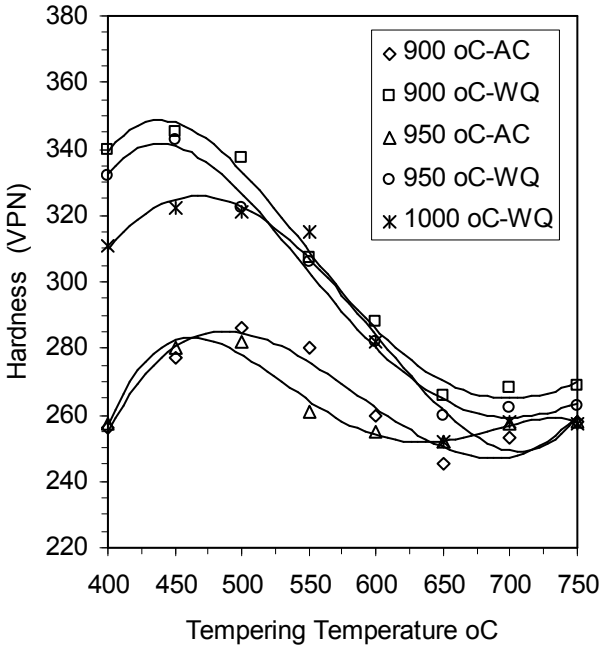

Fig. 3. Hardness vs. tempering temperature curves

It may be observed from Fig. 3 that austenisation temperature did not alter the tempering behaviour of the steel either in water quenched or in air cooled condition. However, there is increase in the as quenched hardness values of the steel with decreasing austenisation temperature. This is due to increased amount of retained austenite in quenched sample owing to austenitisation of the steel at higher temperature. Similar trend was not observed for the steel cooled in air from different austenisation temperatures. The hardness values of the water quenched steel were ranging between 310 - 340 VPN for samples austetinised at different temperatures, whereas the hardness values of the air cooled sample were nearly the same, i.e., 260 VPN at all austetinisation temperatures. The difference in the hardness values of water quenched and air cooled samples is attributed to the difference in the microstructures obtained as a result of different rates of cooling (comparison between Figs. - 4 and 5). As seen from Fig. 4, the microstructure for water quenched steel is acicular in nature, whereas Fig. 5 shows non-polygonal ferritic / Bainitic microstructure in the air cooled sample.

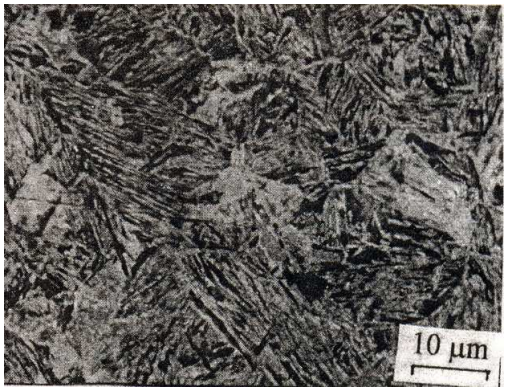

Fig. 4 - SEM of WQ steel

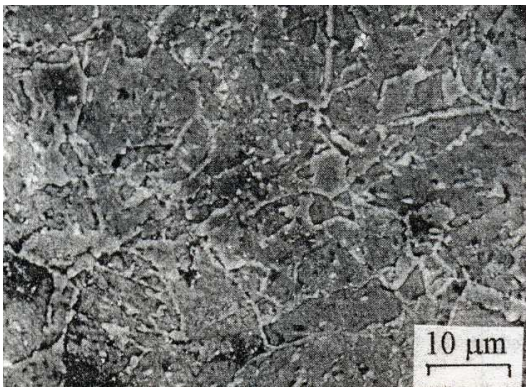

Fig. 5 - SEM of AC steel

The hardness vs. tempering temperature curves show peak values in the vicinity of 450 °C for water quenched samples. Similar peak is also observed for air cooled samples with slight shift of the peak towards higher tempering temperature. The shift of peak for air cooled sample possibly indicates retardation in the kinetics of precipitation for air cooled structure. The probable cause for slight change in the peak temperature is attributed to the difference in the initial microstructure of the water quenched and air cooled samples. Since water quenched and air cooled steel show similar tempering behaviour, it was decided to study quantitative effect of tempering parameters on mechanical properties of water quenched steels only.

The transmission electron microphotographs of the as-quenched (water quenched from 900 °C, 1 hour) samples (Figs. 6a,b) show matrix of lath martensite containing dislocations. On an average the width of the laths was ~0.4 μm as measured in the microscope itself. The areas of austenite region were verified using SAD (typical FCC ring pattern). The region of austenite was further confirmed from dark field image. The continuous rings of SAD pattern were indicative of fineness of the austenite grains. These austenites are the retained austenite in the quenched sample as was observed by various workers [6].

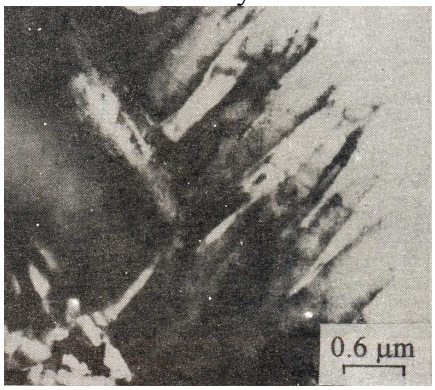

Fig. 6a - TEM of WQ steel showing matrix of lath martensite

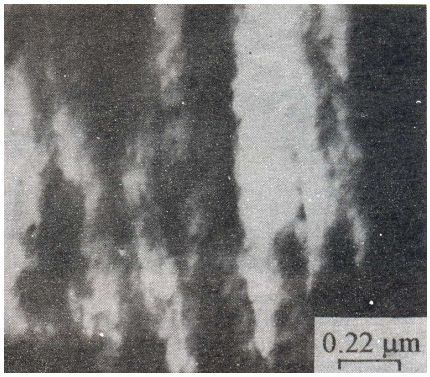

Fig. 6b - TEM of WQ steel showing dislocations

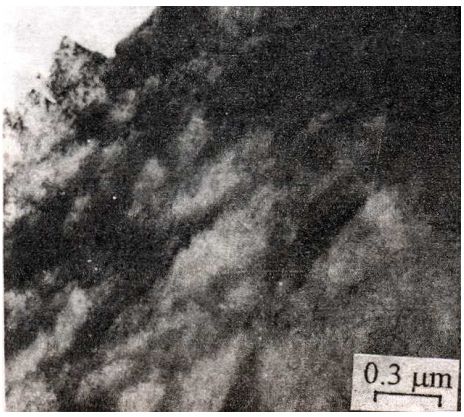

Fig. 7a - TEM of Quenched and tempered steel (450 °C, 1 hour) showing lath structure with dislocations

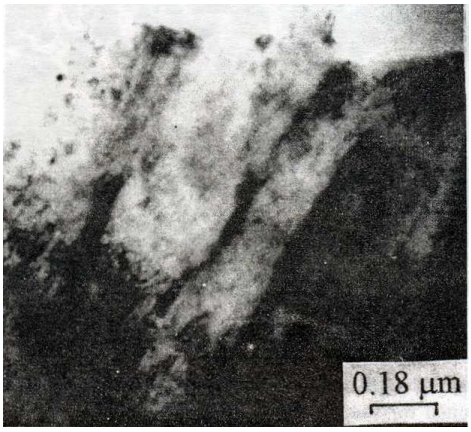

Fig. 7b - TEM of Quenched and tempered steel (450 °C, 1 hour)showing

Figs. 7a,b show the transmission electron microphotographs of quenched and tempered (450 °C, 1 hour) samples. Fig. 7a shows lath structure with dislocations. Fig. 7b is the TEM studies of the same at some other region showing fine precipitates occurring due to tempering.

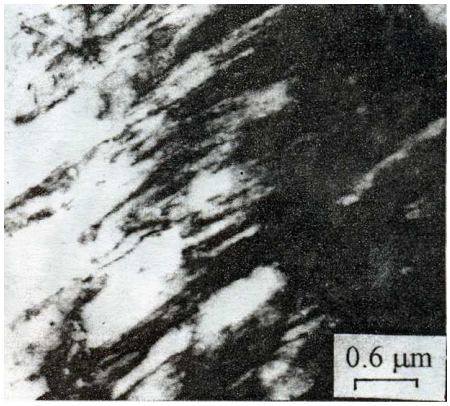

Fig. 8 - TEM of Quenched and tempered steel (600 °C, 1 hour) showing recovered structure

Tempering at 600°C causes recovered structure. TEM photograph (Fig. 8) shows there is less dislocation in the microstructure in white ferritic matrix. Tempering at 700°C resulted recovery of the dislocations in the laths with some precipitates (Fig. 9a). Dark region of second-generation austenite is seen at the lath boundaries (Fig. 9b). The darkness of the austenite is due to quenching of the steel after tempering at 700 °C [5,6].

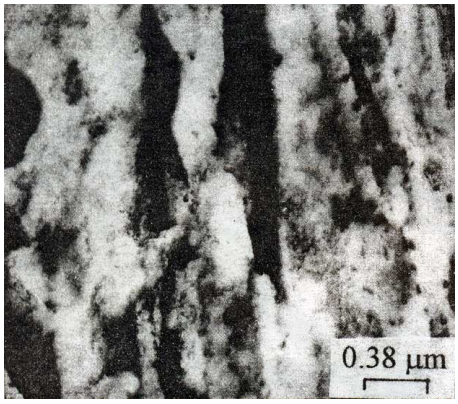

Fig. 9a - TEM of Quenched and tempered steel (700 °C, 1 hour) showing recovery of dislocations with precipitates

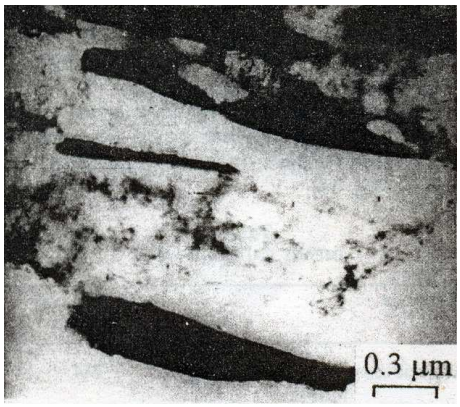

Fig. 9b - TEM of Quenched and tempered steel (700 °C, 1 hour) showing second generation austenite (dark regions) at lath boundaries

Since the steel is designed primarily as a structural material for ship building purpose, the requirement for low-temperature impact properties is very stringent. Therefore, it is necessary to evaluate Charpy values of different heat-treated steels at low temperature before optimization of properties is taken up. Charpy samples used for the above purpose were heat treated as described in Table 3.

Table - 3 . IMPACT VALUES at -50 °C

Treatment	-50 °C CVN value (J)
As recieved	244
(950°C 1hr. - WQ)	122
Air Cool	149
WQ + tempered at 450°C for 1hr.	102
WQ + tempered at 600°C for 1hr.	203
WQ + tempered at 700°C for 1hr.	258

While the Charpy value was the least (102 Joules) for the sample tempered at 450^0C for 1 hr. it was maximum (258 Joules) for the sample tempered at 700^0C for 1 hr. Figs. 10 and 11 represent fractured surfaces of impact test samples tempered at 450 °C and 700 °C respectively. It is evident that while the fractrograph of the former sample (tempered at 450 °C) shows river pattern with quasicleavage areas (typical brittle fracture) (Fig. 10), the later sample (tempered at 700 °C) shows dimples, indicative of typical ductile fracture (Fig. 11).

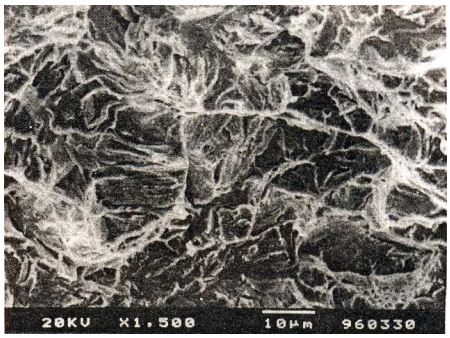

Fig. 10 - Fractograph of broken Charpy specimen (Quenched and tempered at 450 °C, 1 hour) shows quasicleavage nature

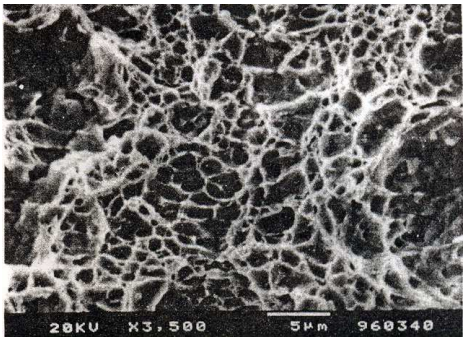

Fig. 11 - Fractograph of broken Charpy specimen (Quenched and tempered at 700 °C, 1 hour) shows dimple fracture

Analysing the results of the impact properties obtained for the heat treated steel, extensive experiments were planned to evaluate mechanical properties of the steel between tempering temperature of 600-700 °C for wide range of tempering time. It may be mentioned here that beyond the tempering temperature of 650 °C, hardness increases (Fig.3). The increase in hardness beyond 650 °C may be explained by the fact that the Ac_1 temperature for this steel being less than 700 °C (Table - 3), the austenite formed at the higher temperature range of tempering, changed to martensite on quenching after tempering (vide dark regions at the lath boundaries in Fig.9b). Further the increase in toughness in this tempering temperature range is attributed to the formation of new generation austenite [6]. Therefore, in the region of tempering temperature of 600 - 700 °C both the impact value and strength value reach optimum condition best suited for use in Naval environment.

Table 4 - Tensile Properties of GPT steel after tempering.

	G P T steel			
Temp °C / Time (hr)	YS MPa	TS MPa	YS/TS	N
700 / 0.33	556.2	662.2	0.85	0.19
700 / 2	483.6	633.7	0.76	0.21
700 / 12	413.0	570.9	0.72	0.25
700 / 80	232.5	341.1	0.68	0.19
600 / 0.33	843.7	853.5	0.99	0.078
600 / 2	708.3	715.1	0.99	0.10
600 / 12	661.2	673.9	0.98	0.09
AQ	867.2	954.5	0.91	-----

Table 4 shows the tensile properties of the steel in different heat-treated conditions. It is seen from the Table that Y.S/T.S ratio of the steel tempered at 700^0C reach a value between 0.68-0.76 whereas for the steel tempered at 600 °C this value remains constant, i.e., 0.98-0.99. Fig. 12 compares typical stress-strain diagram of the steel tempered at 600 °C and 700 °C respectively for 1hr. The stress - strain diagram of steel tempered at 600 °C, shows discontinuous yielding. In contrast, the stress-strain diagram of the steel tempered at 700 °C shows continuous yielding behaviour, typical of a Dual phase steel.

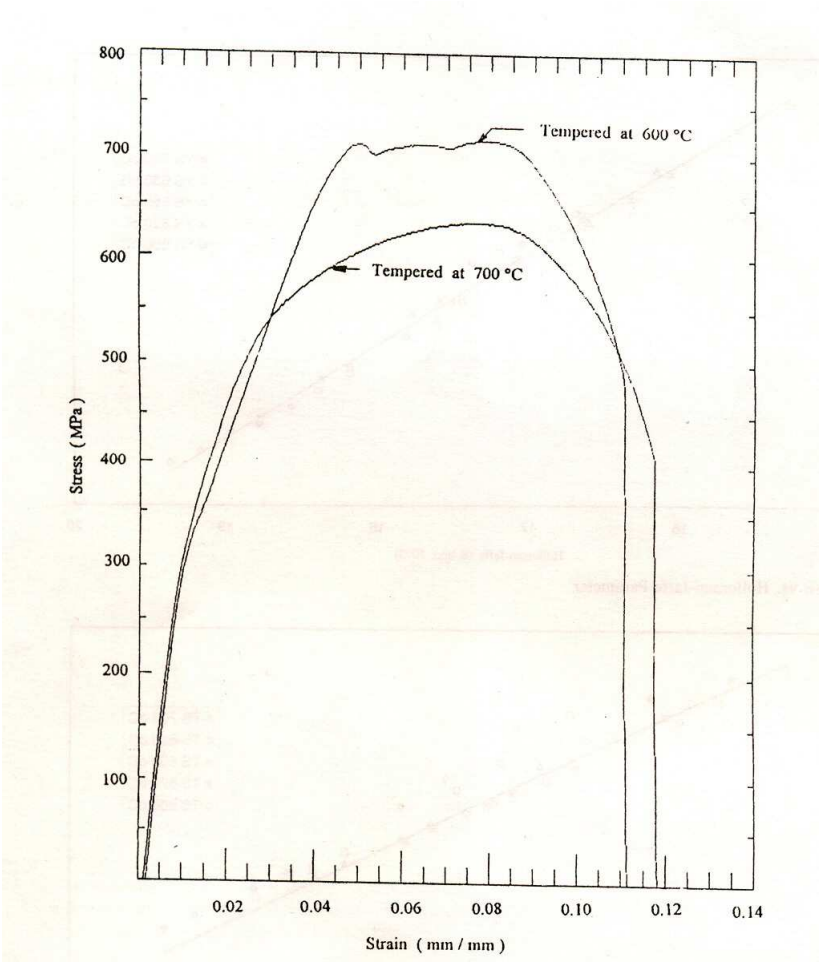

Fig. 12 - Stress-strain diagram of specimens quenched and tempered at 600 °C and 700 °C

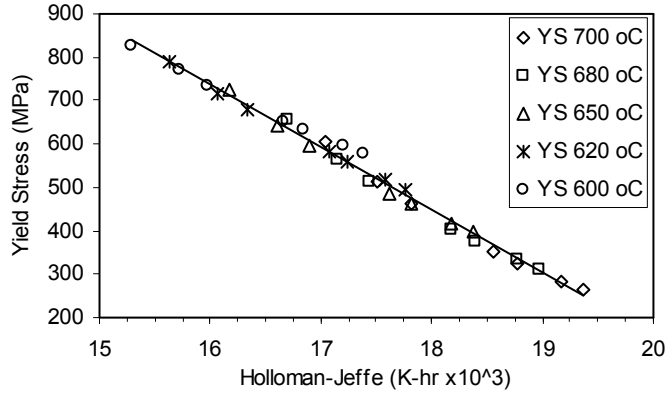

Fig. 13 - YS vs. Hollomon-Jaffe Parameter

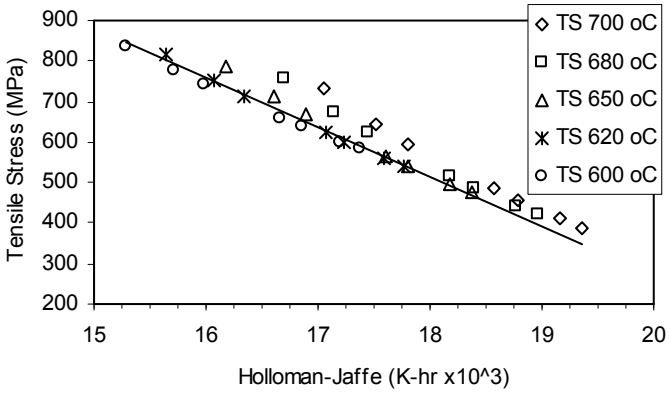

Fig. 14 - UTS vs. Hollomon-Jaffe Parameter

Figs. 13 and 14 show the plot of Holloman-Jaffe temperature normalised parameter with YS and UTS respectively. The YS values fitted well in a straight line with the Holloman-Jaffe parameter at all tempering temperatures as was observed by others [5]. However there is a marked deviation from straight line fit for UTS values while plotted against the parameter, particularly beyond 650 °C of tempering temperature. The possible explanation is attributed to the formation of austenite during tempering above 650 °C. This austenite forms martensite while quenched from tempering temperature and thus forming dual phase microstructure.

The YS and UTS quantified with respect to time and temperature of tempering by Best-fit method are as follows :

$$YS = (2305.105 - 2.5604\ T).\ t^{(3.4589 - 0.551 \ln T)} \quad \text{---------} \quad (1)$$

$$TS = (1528.94 - 1.341\ T).\ t^{(1.994 - 0.322 \ln T)} \quad \text{----------} \quad (2)$$

The equations can be utilised for finding the mechanical properties of the steel for different combinations of time and temperature of tempering. Similar equation is obtained for Charpy value of the steel at -50 °C and is shown below in equation (3) :

$$CVN = (0.03544\ T - 24.3566).t^2 + (-0.52484\ T + 357.7386).t + (1.0706\ T - 493.13) \quad \text{..... (3)}$$

In eqns. (1) to (3), T is tempering temperature in °C and t is the time of tempering in hours. YS and TS are the yield strength and tensile strength in MPa, CVN is the -50 °C Charpy impact value in Joules.

Since it is observed from Tables 3 and 4 that the best combination of properties (YS and -50 °C CVN) occurs in the vicinity of 700 °C and 1 hour time, it was therefore decided to carry out 2^2 factorial design of experiments in this region of time and temperature of tempering. Table 5 shows design matrices for YS and -50 °C CVN value prepared over a tempering temperature range of 600-700 °C and tempering time of 0.33-2 hours. Regression equations for YS and CVN value, which are formed from the design matrices, give quantitative estimate of the properties and can be effectively used for optimization purposes [9,10].

$$YS = 647.95 - 128.05\ X_1 - 52\ X_2 + 15.7\ X_1.\ X_2 \quad \text{..... (4)}$$
$$CVN = 213.75 + 26.75\ X_1 + 15.25\ X_2 - 21.75\ X_1.\ X_2 \quad \text{.....(5)}$$

where $X_1 = (x_1 - 650) / 50$, $X_2 = (x_2 - 1.165) / 0.835$ .....(6)

x_1, x_2 are natural values of temperature and time of ageing and YS is the yeild strength (MPa) and CVN is the Charpy V-notch value at -50 °C (Joule). X_1 and X_2 are in coded form and can be decoded by using the relations given in eqn. (6).

Table 5 - 2^2 Design Matrix along with responses

INPUT VARIABLES		RESPONSES	
Ageing temperature °C	Ageing time (hrs)	YS (MPa)	-50 °C CVN (Joule)
600	0.33	843.7	150
600	2.00	708.3	224
700	0.33	556.2	247
700	2.00	483.6	234

The -ive coefficients of X_1 in eqn.(4) implies that the yield strength will decrease for an increase in tempering temperature above the base level (650 °C $\Rightarrow$ +ive X_1). The +ive coefficient of X_2 in eqn.(5) indicates that there will be increase in Charpy value for +ive X_1. However if $X_1 \Rightarrow 0^+$, then the decrease in YS will be negligible. For decrease in tempering time below the base level (1.165 hours $\Rightarrow$ -ive X_2), the yield strength increases since the coefficient of X_2 in eqn.(4) is –ive. The Charpy value decreases since the coefficient of X_2 in eqn.(5) is +ive. However this decrease is not much since the numerical value of the coefficient of X_2 in eqn.(5) is small and X_2 is a fractional quantity. The effect of the time-temperature interaction is small in both cases since the coefficients of ($X_1.X_2$) are small in eqns. (4) and (5), and two fractional quantities X_1 and X_2 are multiplied. Thus by tempering the steel at a temperature just above the base level (650 °C, i.e., $X_1 \Rightarrow 0^+$) and time near the end of the range ($\Rightarrow$0.33 hours, i.e., $X_2 \Rightarrow 1^-$), there will be some increase in yield strength with high increase in toughness. Thus there is distinct advantage of tempering at a temperature above the base level temperature and time below the base level time.

4. Conclusions

1) The steel responds to tempering both in air cooled and water quenched conditions.
2) Austenitisation at 900 °C followed by quenching in water produces martensitic structure which is distinctly different from the microstructure of austenitised and air cooled steel.
3) Presence of retained austenite is confirmed by SAD and dark field image of TEM microstructure.
4) Maximum strength value and minimum Charpy value at -50 °C are observed by tempering the steel at 450 °C after quenching or air cooling the steel from the austenitisation temperature of 900 °C.
5) The steel shows high value of YS/UTS ratio and discontinuous yielding behaviour after tempering at 600 °C. However, tempering at 700 °C results decreasing YS/UTS ratio with continuous yielding behaviour, typical of Dual Phase steel.
6) The YS and UTS values were plotted against Holloman-Jaffe temperature normalised parameters. The plots of Yield stress vs. Hollomon-Jaffe Parameter show linearity within wider range of tempering temperature. However, similar plots for UTS vs. Hollomon-Jaffe Parameter show significant deviations from linearity at higher tempering temperature. This is due to the formation of austenite at higher tempering temperature.
7) YS and Charpy values have been quantified with respect to time and temperature of tempering in the range of 0.33-12 hours and 600-700 °C respectively by using Best fit method.
8) The quantitative effect of tempering parameters (i.e. temperature and time of tempering) varying in a shorter range are shown in the form of regression

equations obtained by applying statistical Design of Experiments. These quantitative relations are utilised for optimization purpose.

5. References

1. Montemarano T.W., Sach B.P., Gudas J.P., Vassilaros M.G. and Vandervelt H.H., High Strength Low Alloy Steels in Naval Construction, J. Ship Production, 3:145-162, 1986.
2. Steel Plate, Sheet, or Coil, Age-Hardening Alloy, Structural, High Yield Strength (HSLA-80 and HSLA-100), January 1990, MIL-S-24645A(SH).
3. Coldren A.P. and Cox T.B., Development of 100 ksi Yield Steel, Technical Report, David Taylor Research Laboratory, 1985, DTNSRDCN00167-85-C-006.
4. Wilson A.D., Hamburg E.G., Colvin D.J., Thompson S.W. and Krauss G., Properties and Microstructures of Copper Precipitation Aged Plate Steel, Microalloying '88, Chicago, ASM, September 1988.
5. Foley R.P. and Fine M.E., Microstructure and Property Investigation of Quenched and Tempered HSLA-100 Steel, Proc. of Int. Conf. on Processing, Microstructure and Properties of Microalloyed and Other Modern High Strength Low Alloy Steels, Pittsburgh PA, Iron and Steel Society, June 3-6, 1991.
6. Mujahid M., Lis A.K., Garcia C.I. and DeArdo A.J., Structure-Property Studies of Cu-containing HSLA-100 Steels, Proc. of Int. Conf. on Processing, Microstructure and Properties of Microalloyed and Other Modern High Strength Low Alloy Steels, Pittsburgh PA, Iron and Steel Society, June 3-6, 1991.
7. Goodman S.R., Brenner S.S. and Low J.R. Jr., An FIM-Atom Probe Study of the Precipitation of Copper from Iron-1.4 At. Pct. Copper, Part I: Field Ion Microscopy, Metallurgical Transactions, 4A:2363-2369, 1973.
8. Mikalac S.J. and Vassilaros M.G., Strength and Toughness Response to Aging in a High Copper HSLA-100 Steel, Proc. of Int. Conf. on Processing, Microstructure and Properties of Microalloyed and Other Modern High Strength Low Alloy Steels, Pittsburgh PA, Iron and Steel Society, June 3-6, 1991.
9. Panda A.K., Ganguly R.I. and Misra S., Tool and Alloy Steels, March/April (1979), pp 101-108.
10. Hicks C.R., Fundamental Concepts in the Design of Experiments, Holt Rinehart and Winston Inc., New York, (1964).